ARTICLE
Journal of Cellular Biochemistry 111:508–519 (2010)

Journal of Cellular Biochemistry

Dab1 Binds to Fe65 and Diminishes the Effect of Fe65 or LRP1 on APP Processing

Oh Yeun Kwon,[1,2] Kyounghee Hwang,[1,2] Jeom-A Kim,[1] Kwangmyung Kim,[1] Ick Chan Kwon,[1] Hyun Kyu Song,[2] and Hyesung Jeon[1*]

[1]*Biomedical Research Center, Korea Institute of Science and Technology, Seongbuk-gu, Seoul 136-791, Korea*
[2]*School of Life Sciences & Biotechnology, Korea University, Anam-dong, Seongbuk-gu, Seoul 136-701, Korea*

ABSTRACT

Fe65 and Dab1 are adaptor proteins that interact with the cytoplasmic domain of amyloid precursor protein (APP) via phosphotyrosine-binding (PTB) domain and that affect APP processing and Aβ production. Co-expression of Dab1 with Fe65 and APP resumed nuclear translocation of Fe65 despite of its cytoplasmic anchor, APP. The decreased amount of Fe65 bound to APP was shown in co-immunoprecipitation assay from the cells with Dab1 which also displayed the effect on APP processing. These data suggested that Fe65 and Dab1 compete for binding to APP. Surprisingly, we found that Fe65 interacts with Dab1 via C-terminal region of Dab1 and unphosphorylated Dab1 is capable of binding Fe65. Dab1 interacts with the low-density lipoprotein receptor-related protein (LRP) as well as APP through its PTB domain. Dab1 significantly decreased the amount of APP bound to LRP and the level of secreted APP and APP-CTF in LRP expressing cells, unlike Fe65. It implies that overexpression of Dab1 diminish LRP–APP complex formation, resulting in altered APP processing. The competition for overlapped binding site among adaptor proteins may be related to the regulation mechanism of APP metabolism in various conditions. J. Cell. Biochem. 111: 508–519, 2010.

KEY WORDS: Dab1; Fe65; PHOSPHOTYROSINE-BINDING DOMAIN; NPTY MOTIF; APP PROCESSING; LRP

Amyloid precursor protein (APP) is a type I membrane protein and is the precursor of amyloid β-peptide (Aβ), the principal component of senile plaques, which is a pathological hallmark in Alzheimer disease (AD) brains. The production, aggregation, and deposition of Aβ are widely believed to be central to the pathogenesis in AD [Gandy, 2005]. APP undergoes extracellular cleavage by α- or β-secretase, resulting in the formation of a large N-terminal extracellular fragment (APPs) and smaller, membrane-bound C-terminal fragments (CTF). If the initial cleavage event occurs via β-secretase, then cleavage of CTF by γ-secretase results in the formation of Aβ [Hoe et al., 2005]. The cytoplasmic domain of APP possesses the NPTY motif to which several phosphotyrosine-binding (PTB) domain-containing proteins bind, such as members of the Fe65, X11, JIP, and Dab protein families [Parisiadou and Efthimiopoulos, 2007]. These proteins play critical roles in tyrosine kinase-mediated signal transduction, protein trafficking, phagocytosis, cell fate determination, and neuronal development [King and Scott Turner, 2004].

The effects on APP trafficking and processing of several adaptor proteins have been studied. The Fe65 family (Fe65, Fe65L1, and Fe65L2) is expressed at high level in neurons [Guenette et al., 2002; Chang et al., 2003]. All three members contain a WW domain and two PTB domains, which display distinct binding specificities. The WW domain binds Mena (mammalian enabled), functioning in regulation of the actin cytoskeleton, cell motility, and neuronal growth cone formation [Ermekova et al., 1997; Sabo et al., 2001]. The interaction between Fe65 and APP is mediated via the PTB2 domain of Fe65 and modulates APP processing and trafficking in several cell lines [Borg et al., 1996; Guenette et al., 1999; Santiard-Baron et al., 2005]. In HEK293 cells, Fe65 stabilizes immature APP and inhibits APPs formation and Aβ secretion [Ando et al., 2001]. APP serves to tether Fe65 to cytoplasmic membranes [Minopoli

Abbreviations used: Dab1, disabled 1; APP, amyloid precursor protein; Aβ, amyloid β; AD, Alzheimer disease; CTF, C-terminal fragments; PTB, phosphotyrosine binding; Mena, mammalian enabled; AICD, APP intracellular domain; LRP, low-density lipoprotein receptor-related protein; apoEr2, apolipoprotein E receptor 2; VLDLR, very low-density lipoprotein receptor; ITC, isothermal titration calorimetry.

Grant sponsor: Ministry of Education, Science & Technology, Korea; Grant sponsor: Korean Government (MEST).

*Correspondence to: Hyesung Jeon, Biomedical Research Center, Korea Institute of Science and Technology, Seoul 136-791, Korea. E-mail: hjeon@kist.re.kr

Received 10 December 2009; Accepted 2 June 2010 • DOI 10.1002/jcb.22738 • © 2010 Wiley-Liss, Inc.
Published online 21 June 2010 in Wiley Online Library (wileyonlinelibrary.com).

et al., 2001]. After sequential proteolytic processing of membrane-bound APP and release of APP intracellular domain (AICD) to the cytoplasm, Fe65 can translocate to the nucleus to participate in gene transcription events [Kinoshita et al., 2002; Cao and Sudhof, 2004]. The Fe65 PTB1 domain interacts with the low-density lipoprotein receptor-related protein (LRP) [Gotthardt et al., 2000]. LRP1 is a large type I transmembrane protein whose small cytoplasmic tail contains two NPXY motifs [Herz and Strickland, 2001]. Fe65 acts as a cytoplasmic linker between LRP and APP [Kinoshita et al., 2001; Pietrzik et al., 2004].

The Dab family members Dab1 and Dab2 are important for nervous system development [Bar et al., 2000]. These proteins possess a PTB domain and have been shown to interact with APP and apolipoprotein E receptor 2 (apoEr2) [Gotthardt et al., 2000]. Dab1 is tyrosine phosphorylated during embryogenesis and responsible for the correct positioning of neurons within laminar structures throughout the brain, functioning as part of the Reelin signaling pathway [Howell et al., 1997b]. Upon neuronal positioning signals, Reelin binds to apoEr2 and the very low-density lipoprotein receptor (VLDLR) resulting in tyrosine phosphorylation of Dab1, and in the subsequent initiation of an intraneuronal signaling cascade [Howell et al., 1997a, 2000]. Recent studies reported that Dab1 interaction with APP and apoEr2 increases levels of their secreted extracellular domains and cytoplasmic C-terminal fragments. These effects depend on the NPTY motif of APP and apoEr2, and on the PTB domain of Dab1 [Hoe et al., 2006b].

The effects of adaptor proteins leading to different pathways are not well understood so far, especially on APP trafficking and processing. Since both Fe65 and Dab1 bind to the NPTY motif on the cytoplasmic domain of APP, we tested whether Fe65 and Dab1 compete for interaction with the cytoplasmic domain of APP and examined the functional consequences of this competition. In this study, we demonstrated that Dab1 affects the binding between of Fe65 and APP, furthermore APP processing. Fe65 anchored to the cytoplasm by its association with APP was released and translocated into the nucleus by Dab1 co-expression. Dab1 also significantly decreased the interaction between LRP and APP, and APP processing through its PTB domain. Interestingly, it was found that Fe65 interacts with Dab1 and this interaction occurs via C-terminal region of Dab1. As there are several adaptor proteins for a binding site, the interaction among adaptor proteins might be involved in the regulation of trafficking and processing of APP.

MATERIALS AND METHODS

PLASMID CONSTRUCTION

To make HA-tagged construct for APP695, human APP695 cDNA lacking the termination codon was generated by PCR and inserted into the *Hin*dIII–*Xho*I sites of modified pcDNA3 expression vector (Invitrogen) containing 3-HA epitope-tags. Construct of APP-CFP was generated by PCR and inserted into the *Hin*dIII–*Sac*II sites of pECFP-C1 (Clontech). APP695 in pDsRed2-N1 (Clontech) was also constructed in a similar manner (APP-RFP). A deletion mutant lacking NPTY motif (amino acids 676-695) of APP695 was generated by PCR and inserted into the *Hin*dIII–*Sac*II sites of pECFP-C1 (Clontech) or pDsRed2-N1 (Clontech) to generate mAPP-CFP and mAPP-RFP. The cDNA encoding full-length mouse Dab1 was PCR amplified and inserted into the *Hin*dIII–*Xho*I sites of modified pcDNA3 expression vector (Invitrogen) containing 3-Myc epitope-tags. To make CFP fused construct for Dab1, Dab1 cDNA was generated by PCR and inserted into the *Xho*I–*Bam*HI sites of pECFP-C1 (Clontech) in frame (Dab1-CFP). Dab1 in pEGFP-C1 (Clontech) was also constructed in a similar manner (Dab1-GFP). A deletion mutant lacking PTB domain (amino acids 1–189) of Dab1 was generated by PCR and inserted into the *Hin*dIII–*Sac*II sites of pECFP-C1 (Clontech) to generate a Dab1-CTF-CFP. The following deletion constructs of Dab1 were produced by PCR and inserted into the *Hin*dIII–*Xho*I sites of modified pcDNA3 expression vector (Invitrogen) containing 3-HA epitope-tags; Dab1-PTB (amino acids 1–189), Dab1-CTF (amino acids 190–555), Dab1-ΔpTyr (amino acids 233–555). The cDNA encoding rat Fe65 was inserted into the pcDNA3 expression vector (Invitrogen) at the *Hin*dIII–*Xba*I sites to produce a C-terminal FLAG fusion protein. To make a GFP fused construct for Fe65, Fe65 cDNA was generated by PCR and inserted into the *Hin*dIII–*Sac*II sites of pEGFP-C1 (Clontech) in frame (Fe65-GFP). To make a Myc-tagged construct for LRP, 3-Myc fused C-terminal fragment (amino acids 4065–4544) of LRP was amplified by PCR and inserted into *Hin*dIII site of pcDNA3.1-LRP plasmid containing the human LRP cDNA. Recombinant DNAs were confirmed by sequencing and the expression of correctly sized proteins was verified by immunoblotting.

PURIFICATION OF RECOMBINANT PROTEINS

Fe65 or Dab1-CTF was inserted into pET22b expression vector (Novagen) to generate 6-histidines fusion proteins. The constructs were transformed in *Escherichia coli* BL21(DE3) cells, and the expression was induced by adding 1 mM IPTG at 18°C. Recombinant proteins were overexpressed as soluble forms, and they were purified using Ni^{2+}-chelated column (Amersham Bioscience). The proteins were further purified using Q-Sepharose ion-exchange column and gel filtration on a HiLoad 26/60 Superdex-75 or Superose 6 prep-grade column. All steps were carried out at 4°C. The purified proteins were concentrated using Amicon concentrator and stored at −80°C until use.

CELL CULTURE AND TRANSFECTIONS

COS7 and HEK293 cells were maintained in Dulbeccos's modified Eagle medium (Invitrogen) with 10% fetal bovine serum (FBS), 100 U/ml of penicillin, 100 μg/ml of streptomycin at 37°C in 5% CO_2. Transient transfection of the cells was performed using Lipofectamine (Invitrogen) according to the manufacturer's instructions.

ANTIBODIES

The used antibodies are; anti-HA (Santa Cruz), anti-Myc (Santa Cruz), anti-FLAG (M2, Sigma), anti-Dab1 (Chemicon), anti-Fe65 (Abcam), anti-phosphotyrosine (4G10, Upstate), anti-tubulin (Sigma), anti-c-jun (Santa Cruz). For analysis of APP, we used anti-APP (6E10 recognizing APP, sAPPα, and β-CTF, Signet), polyclonal anti-APP cytoplasmic domain 8717 (Sigma), and monoclonal anti-APP extracellular domain 22C11 (Chemicon) antibodies.

CO-IMMUNOPRECIPITATION

For the immunoprecipitation experiments, cell extracts were incubated with appropriate dilutions of the various antibodies overnight at 4°C. Antibody-bound protein complexes were collected with protein G-Sepharose beads (Amersham Biosciences) for 1 h at 4°C, and then the precipitates were washed four times with lysis buffer (50 mM Tris–HCl, pH 8.0, 0.15 M NaCl, 1% Nonidet P-40, and protease inhibitor cocktail (Sigma)). The beads were resuspended in SDS sample buffer (0.4 M SDS, 0.4 M Tris, 40 mM EDTA, 50% glycerol, bromophenol blue) and the samples were separated by SDS–PAGE gel electrophoresis, and detected by immunoblot analysis.

IMMUNOBLOTTING

Forty-eight hours after transfection, cell extracts or conditioned media were removed and centrifuged at 15,000*g* for 10 min at 4°C to discard cellular debris. Cells were lysed at 4°C in lysis buffer (50 mM Tris–HCl, pH 8.0, 0.15 M NaCl, 1% Nonidet P-40) supplemented with complete protease inhibitor cocktail (Sigma). Following 30 min incubation on ice, protein extracts were clarified by centrifugation at 15,000*g* for 30 min at 4°C. Cell extracts and conditioned media samples were separated by SDS–PAGE gel electrophoresis, and transferred to polyvinyldiene difluoride (PVDF) membranes (Millipore). Membranes were blocked in Tris-buffered saline containing 0.1% Tween-20 and 5% nonfat dried milk and subjected to the incubation with primary antibodies at room temperature for 1 h. Horseradish peroxidase-conjugated secondary antibodies were used for visualization by ECL detection system (Amersham Biosciences). Three independent experiments were performed and the standard deviations were calculated for the quantification graph of the blot.

SUBCELLUAR FRACTIONATION

Subcelluar fractionation of cells was performed using ProteoExtract Subcellular Proteome Extraction Kit (Merck) according to the manufacturer's instructions and the purity of the different fractions determined by probing with fraction-specific markers (tubulin and c-Jun).

FLUORESCENCE MICROSCOPY

Microscopy was performed on a DeltaVision system manufactured by Applied Precision (Issaquah, WA). The sample was imaged using a microscope (IL-70, Olympus) equipped with a 100 W mercury arc lamp, a Uplan Apo 60X oil objective (1.35 numerical aperture), a CoolSnap HQ digital camera from Roper Scientific (Tucson, AZ) and optical filter sets from Omega Optical (Brattleboro, VT). COS7 cells were plated on glass-bottomed dishes and transfected with 1 μg of each plasmid. Twenty-four hours after the transfection, cells were observed with a 60× oil immersion objective lens equipped on the fluorescence microscope. Intermediately bright cells were chosen for imaging experiments. Exposure time was 200 ms with 2 × 2 binning and the final image size was 512 × 512. The system was operated with the CFP filters (excitation 436 nm, emission 470 nm), the FITC filters (excitation 490 nm, emission 528 nm), and the Rhodamine filters (excitation 570 nm, emission 590 nm) independently. Images were analyzed with the SoftWoRx program from Applied Precision.

ITC MEASUREMENTS

Isothermal titration calorimetry (ITC) measurements were performed on a MicroCal VP-ITC 200 isothermal titration calorimeter (MicroCal, Inc.). PIPES buffer (20 mM PIPES buffer, pH 7.0, 150 mM NaCl) was used for the ITC measurements at 25°C. The purified Fe65 was diluted to a concentration of 0.01 mM in the PIPES buffer and placed in the sample cell. The purified Dab1-CTF was diluted to a concentration of 0.15 mM in the PIPES buffer and placed in the injection syringe. For each titration, 1.5 μl aliquots of Dab1-CTF were delivered under computer control into the Fe65 solution at 150 s intervals to allow complete equilibration. The heat of dilution, obtained by titrating the identical Dab1-CTF solution into the reaction cell containing only the PIPES buffer, was subtracted prior to analysis. The corrected titration curve was fitted with a one-site model, and the thermodynamic parameters were calculated using the Origin software (version 7.0) provided by MicroCal, Inc.

RESULTS

CELLULAR LOCALIZATION OF Fe65 WITH APP IS AFFECTED BY Dab1 CO-EXPRESSION

The NPTY motif on APP cytoplasmic tail is a consensus sequence for binding of proteins such as Fe65 and Dab1 via their PTB domain [Hoe and Rebeck, 2008]. Structural studies of APP peptide–PTB domain complexes revealed similar binding positions among different adaptor proteins on the interaction with APP [Li et al., 2008; Radzimanowski et al., 2008]. There is a report that X11 competes with Fe65 for binding to APP [Lau et al., 2000], which seems to be obvious from the superposition of binding peptides on these proteins. We examined the effect of Dab1, another adaptor protein, on the interaction of Fe65 with APP in cells. Fe65 can translocate to the nucleus to participate in gene transcription events [McLoughlin and Miller, 2008]. We first confirmed that Fe65 is anchored in the cytoplasm by its association with the APP when these two proteins are co-expressed in the cells as known in previous studies [Cao and Sudhof, 2001; Minopoli et al., 2001]. To check that APP regulates the cellular distribution of Fe65 in our system, we transfected COS7 cells with the GFP fused Fe65 (Fe65-GFP) and the CFP fused APP (APP-CFP), and examined the subcellular distribution of Fe65 and APP using fluorescence microscopy. In single transfected cells, APP-CFP is localized in the cytoplasm excluded from the nucleus, whereas Fe65-GFP is localized in both the nucleus and cytoplasm as reported (Fig. 1A, a,b). Co-expression with APP-CFP tethered Fe65-GFP in the cytoplasm, showing co-localization (Fig. 1A, e–g). When Fe65-GFP was co-expressed with mutant APP-CFP lacking the NPTY motif that is unable to bind Fe65-GFP, it resumed largely nuclear localization (Fig. 1A, h–j). Consistent with previous reports [Cao and Sudhof, 2001; Minopoli et al., 2001], we obtained data showing that overexpressed APP tethers most of the Fe65 in the cytoplasm through the NPTY motif.

We examined the possibility that co-expression of Dab1 altered Fe65 translocation to nucleus. Expression vector was prepared for the CFP fused Dab1 (Dab1-CFP) and it was co-transfected with Fe65-GFP into COS7 cells. In single transfected cells, Dab1-CFP was detected throughout the cytoplasm (Fig. 1A, d). In COS7 cells co-

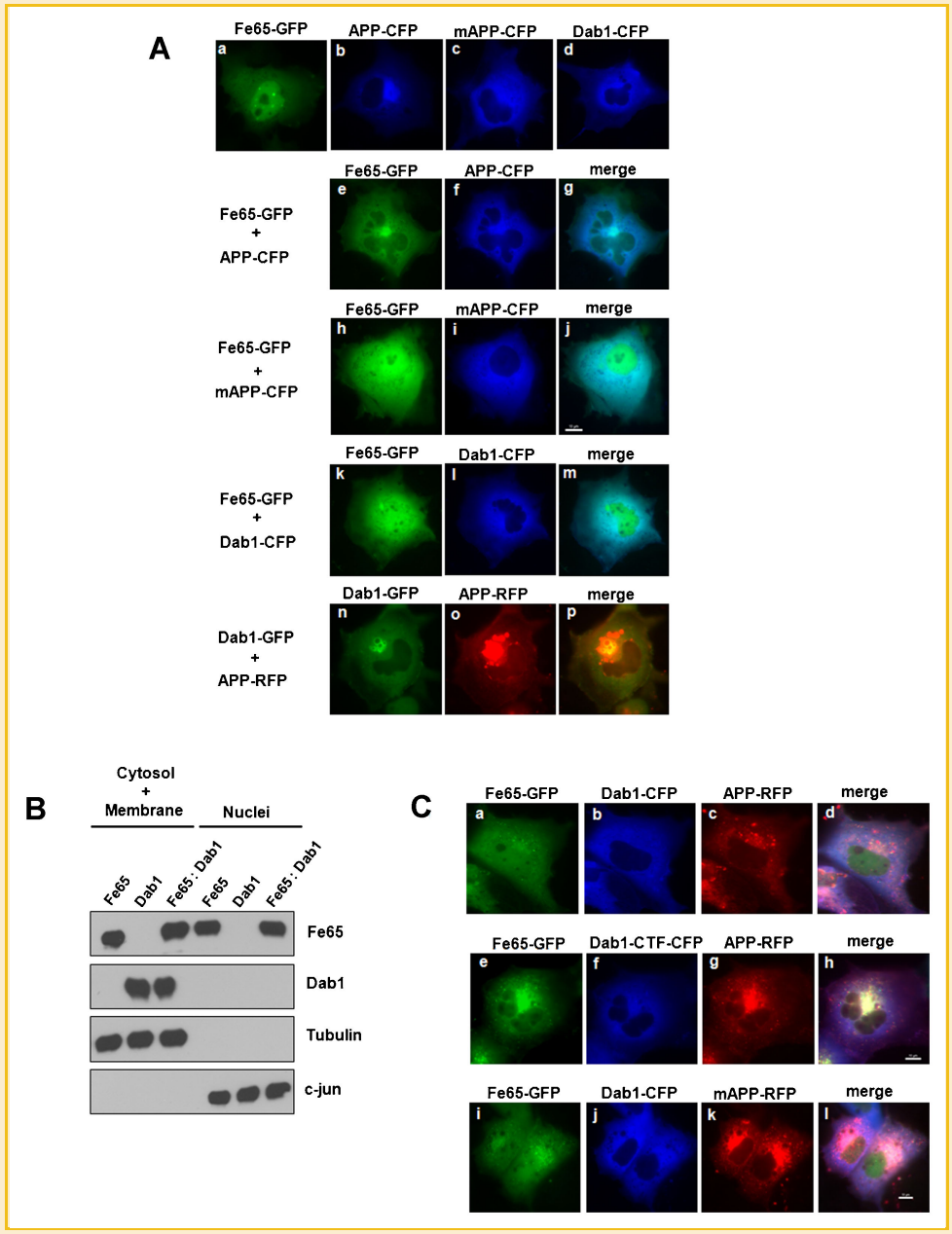

Fig. 1. The effect of APP on nuclear translocation of Fe65 in the presence of Dab1. A, a–d: Cellular localization of Fe65, APP, mutant APP lacking the NPTY motif (mAPP), or Dab1. COS7 cells were individually transfected with Fe65-GFP, APP-CFP, mAPP-CFP, or Dab1-CFP. e–m: Localization of Fe65 in the presence of APP, mAPP, or Dab1. APP-CFP, mAPP-CFP, or Dab1-CFP were co-transfected with Fe65-GFP. n–p: Localization of Dab1 in the presence of APP. COS7 cells were co-transfected with Dab1-GFP and APP-RFP. B: Subcellular fractionations of Fe65, Dab1, and Fe65 + Dab1 transfected COS7 cells. The combined cytoplasmic and membrane, and the nuclear fractions were probed with antibodies for Fe65, Dab1, and subcellular fraction-specific markers, tubulin and c-jun. C, a–d: Cellular localization of Fe65 in the presence of Dab1 and APP. COS7 cells were co-transfected with Fe65-GFP, Dab1-CFP, and APP-RFP. In cells co-expressing Fe65, Dab1, and APP, Fe65 was localized primarily to the nucleus as well as in the cytoplasm (a). This translocation to the nucleus of Fe65-GFP was not inhibited by APP in the presence of Dab1. e–h: Localization of Fe65 in the presence of Dab1-CTF lacking the PTB domain and APP. COS7 cells were co-transfected with Fe65-GFP, Dab1-CTF-CFP, and APP-RFP. When Fe65 and APP were expressed with Dab1-CTF that is unable to bind APP, Fe65 largely localized to the cytoplasm by APP (e). i–l: Localization of Fe65 in the presence of Dab1 and mAPP. COS7 cells were co-transfected with Fe65-GFP, Dab1-CFP, and mAPP-RFP. In cells co-expressing Fe65, Dab1, and mAPP, Fe65 was localized in both the nucleus and cytoplasm (i). Because mAPP is unable to bind both Fe65 and Dab1, mAPP had no effect on Fe65 translocation to nucleus.

transfected with Fe65-GFP and Dab1-CFP, Fe65-GFP is located in the nucleus and cytoplasm (Fig. 1A, k–m). There was no noticeable difference in the distribution of Fe65 in the presence or absence of Dab1. To confirm this distribution, we separated nuclear and cytosolic/membrane fractions from the transfected cells and probed for the presence of Fe65 and Dab1 by immunoblotting. Fe65 was present in both cytosol/membrane and nuclear fractions but Dab1 was present only in cytosol/membrane fractions (Fig. 1B). These

results showed that Dab1 does not significantly affect nuclear translocation of Fe65, unlike APP tethering in the cytoplasm.

Dab1 contains a PTB domain, which have been shown to interact with the cytoplasmic domain of APP and is a nucleocytoplasmic shuttling protein. It raises a possibility that Dab1 might play a role in the nucleus as well as in the cytoplasm [Honda and Nakajima, 2006]. Therefore, we investigated the possibility that co-expression of APP altered Dab1 cellular localization. The GFP fused Dab1 (Dab1-GFP) was co-transfected into COS7 cells with the RFP fused APP (APP-RFP). When Dab1-GFP was co-expressed with APP-RFP, Dab1-GFP was still localized in the cytoplasm as APP-RFP (Fig. 1A, n–p). These results suggest that co-expression of APP could not affect cellular localization of Dab1. Translocation was shown only in the case for co-transfection of APP and Fe65.

Then, we studied the effect of APP on nuclear translocation of Fe65 in the presence of Dab1. The Fe65-GFP was co-transfected into COS7 cells with Dab1-CFP and APP-RFP. In Fe65-GFP/Dab1-CFP/APP-RFP triple transfected COS7 cells, Fe65-GFP is localized in the nucleus (Fig. 1C, a–d). Compared to the co-transfection of APP with Fe65 in which most Fe65 was localized in the cytoplasm by APP (Fig. 1A, e–g), co-transfection of Dab1 with APP and Fe65 made Fe65 remain in the nucleus (Fig. 1C, a). This result suggests the disruption of interaction between Fe65 and APP by Dab1. To support this, we generated an expression vector that encodes a CFP-fused deletion mutant of Dab1 (Dab1-CTF-CFP) that lacks the PTB domain which is responsible for binding APP. In Fe65-GFP/Dab1-CTF-CFP/APP-RFP triple transfected COS7 cells, Fe65-GFP was localized in the cytoplasm (Fig. 1C, e–h). Because Dab1 mutant is unable to interact with APP [Hoe et al., 2006b], APP binds Fe65 to localize it in the cytoplasm. When Fe65-GFP and Dab1-CFP were expressed with mAPP-RFP that lacks the NPTY motif, Fe65-GFP was localized in the nucleus again (Fig. 1C, i–l). The deletion mutant of APP (mAPP-RFP) probably abrogates binding of Dab1 as well as Fe65 as shown in Figure 1A. These results show that Dab1 interactions with APP reduced the amount of Fe65 bound to APP, thus the liberated Fe65 from cytoplasm was translocated into the nucleus.

THE EFFECT OF Fe65 AND Dab1 CO-EXPRESSION ON THEIR INTERACTION WITH APP AND ON APP PROCESSING

The amount of Fe65 co-precipitated with APP in the absence or presence of Dab1 was determined using immunoprecipitation. Notably, the amount of Fe65 bound to APP was decreased in the presence of Dab1 as expected from the fluorescent images (Fig. 2A). We next performed the reverse, determining the amount of Dab1 co-precipitated with APP in the absence or presence of Fe65. The amount of Dab1 bound to APP was also decreased in the presence of Fe65 (Fig. 2B). Western blot analysis of cell extracts confirmed that levels of total APP were consistent across the transfections. These results confirm that Fe65 compete with Dab1 for binding to APP.

It was reported that Fe65 stabilizes immature APP and inhibits sAPP and Aβ secretion in HEK293 cells [Ando et al., 2001]. On the other hand, Dab1 increases cellular levels of mature APP and this increase is paralleled by an increase in the secretion of sAPP and Aβ [Parisiadou and Efthimiopoulos, 2007]. In order to examine the effect of Fe65 and Dab1 co-expression on the APP processing, HEK293 cells were transiently co-transfected with APP, Fe65, and Dab1. Secreted APP was measured in the conditioned media, and APP-CTF was measured in cell lysates (Fig. 2C). As previously demonstrated by others, it showed that Dab1 increased secreted APP and APP-CTF in co-transfected HEK293 cells with APP and Dab1 (Fig. 2C, lane 3). In contrast, Fe65 significantly decreased secreted APP and APP-CTF in co-transfected HEK293 cells with APP and Fe65 (Fig. 2C, lane 2). In the presence of Fe65, co-expression with Dab1 partly restored levels of secreted APP and APP-CTF compared with cells transfected with APP and Fe65 (Fig. 2C, lane 1). Levels of total APP in cell extracts were consistent across the transfections (Fig. 2C, bottom panel). These results indicate that Fe65 and Dab1 exert opposing effects on APP processing and Dab1 decreases the effect of Fe65 on APP processing, possibly by competing for binding APP.

Dab1 INTERACTS WITH Fe65 THROUGH ITS C-TERMINAL PART

To explore the possibility of interaction between Fe65 and Dab1 after confirming their competition toward APP binding, we examined co-precipitation of Fe65 and Dab1 using antibodies for different tagging. Dab1 was co-precipitated with Fe65 but was not precipitated in the absence of Fe65 or Dab1 (Fig. 3A). Western blotting of cell extracts confirmed that levels of total Fe65 and Dab1 were consistent across transfections. We also performed the reverse experiment, immunoprecipitating Dab1, and probing with anti-FLAG antibody for Fe65. Fe65 was co-precipitated with Dab1 but was not precipitated in the absence of Fe65 or Dab1 (Fig. 3B). In order to test whether this interaction was merely from the forced overexpression of proteins, we examined whether native Fe65 and Dab1 interact each other in the mouse brain lysates. We carried out the same pull-down experiments with mouse brain lysates. Dab1 resulted in co-precipitation with Fe65 and vice versa (Fig. 3C). HEK293 cells used in our experiments do not have endogeneous APP nor LRP, at least in the level for Western blotting detection, which supports the direct binding of Fe65 and Dab1 (data not shown).

We generated expression vectors to determine which domain of Dab1 interacts with Fe65; HA-tagged constructs of Dab1, Dab1-PTB (N-terminal region of amino acid 1–189) lacking the C-terminus of Dab1, and Dab1-CTF (C-terminal region of amino acid 190–555) lacking the PTB domain (Fig. 4A). They were co-transfected with the Fe65 tagged by FLAG into HEK293 cells, and their lysates were subjected to immunoprecipitation with anti-HA antibody followed by immunoblotting with anti-FLAG antibody. Proteins of expected sizes were expressed to similar levels from each Dab1 construct, as determined by Western blot analysis (Fig. 4B). Fe65 was co-precipitated with Dab1-CTF but not the Dab1-PTB (Fig. 4B). These results indicate that the C-terminus of Dab1 contributes to the binding Fe65.

The dissociation constants of the complex between Dab1-CTF and Fe65 were measured directly by ITC using the purified recombinant proteins. The upper panel of Figure 4C shows the heat of reaction for about 27 titrations of Dab1-CTF into the Fe65 solution at 25°C. The binding reaction is exothermic, and the integrated heats of reaction are shown in the lower panel of Figure 4C. Assuming a 1:1 binding model, a nonlinear least squares fit of the binding curve provides values for the stoichiometry of binding (n) of 1. The K_d between

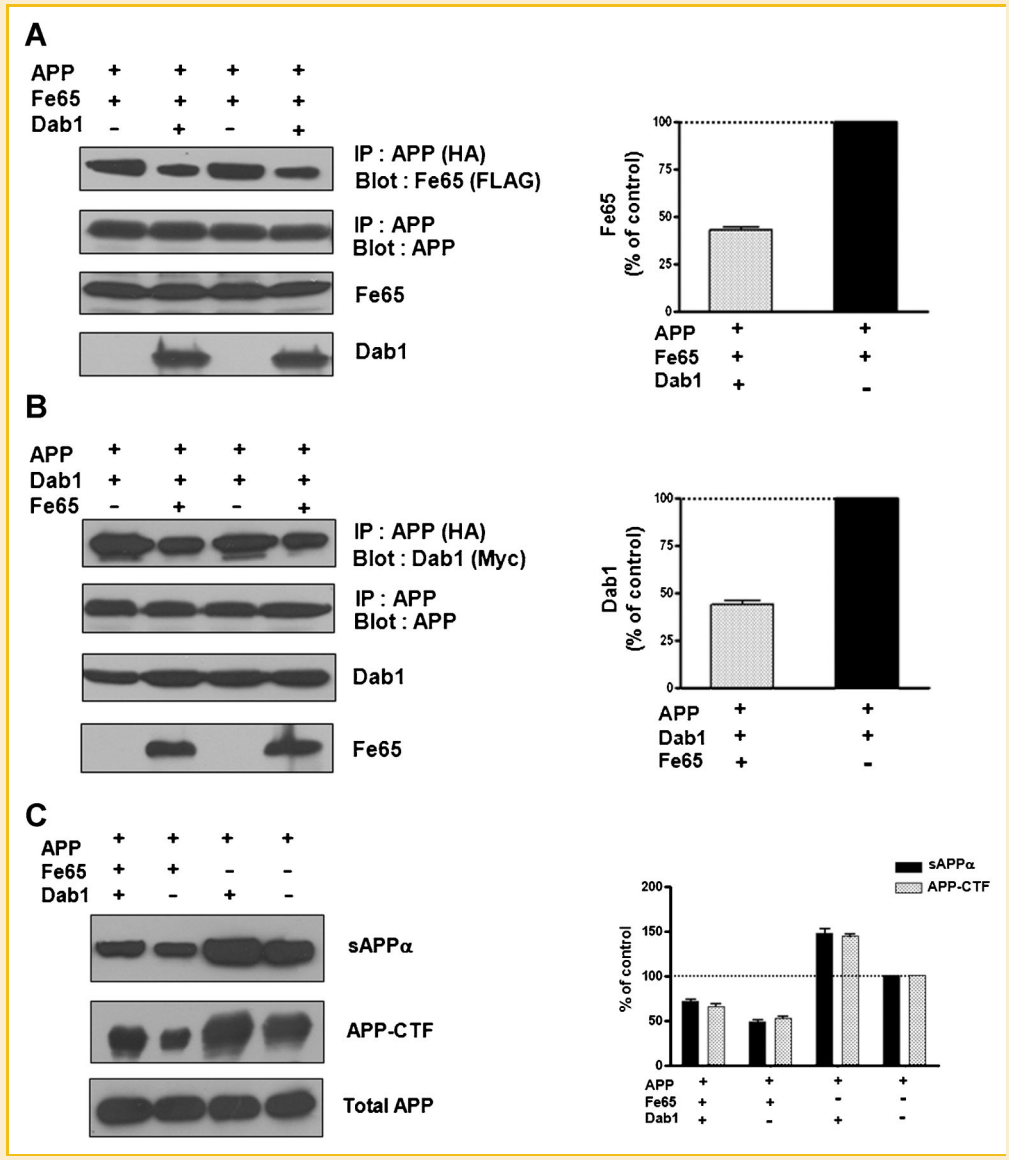

Fig. 2. The effect of the co-expression of Fe65 and Dab1 on their interaction with APP and APP processing. A: HEK293 cells were co-transfected with APP and Fe65 without or with Dab1. Cell lysates were immunoprecipitated with anti-HA antibody, and the precipitate was probed with anti-FLAG antibody. Dab1 decreased co-precipitation of Fe65 and APP (top panel). Immunoblots of cell lysates showed similar levels of total APP and Fe65 (lower panels). Three independent experiments were performed and the standard deviations were calculated for the quantification graph of the blot. B: HEK293 cells were co-transfected with APP and Dab1 without or with Fe65. Cell lysates were immunoprecipitated with anti-HA antibody, and the precipitate was probed with anti-Myc antibody. Fe65 decreased co-precipitation of Dab1 and APP (top panel). Immunoblots of cell lysates showed similar levels of total APP and Dab1 (lower panels). Three independent experiments were performed and the standard deviations were calculated for the quantification graph of the blot. C: HEK293 cells were co-transfected with APP and Fe65, Dab1 (lane 1), APP and Fe65 (lane 2), APP and Dab1 (lane 3), APP (lane 4). Secreted APPα was measured in conditioned medium with 6E10 antibody (upper panel), and APP-CTF was measured in cell lysates with 8717 antibody (middle panel). Immunoblot of cell lysates showed similar levels of total APP (lower panel). Three independent experiments were performed and the standard deviations were calculated for the quantification graph of the blot.

Dab1-CTF and Fe65 was ~5.8 μM. This result confirms that the Fe65 and Dab1 interact also in vitro.

After examining which domain of Dab1 interacts with Fe65, we investigated whether the tyrosine phosphorylation of Dab1 is involved in the binding to Fe65. The residues 198, 200, 220, and 232 of Dab1 are tyrosine-phosphorylated in response to Reelin and mediate the interaction with downstream signaling molecules [Howell et al., 2000; Stolt and Bock, 2006]. We made HA-tagged deletion mutant of Dab1-CTF (Dab1-ΔpTyr) that lacks residues Glu190-Tyr232 including four tyrosines mentioned above (Fig. 4A). Fe65 co-precipitated with Dab1-ΔpTyr in HEK293 cells expressing both Dab1-ΔpTyr and Fe65 (Fig. 4D). The Dab1 bound to Fe65 regardless of the deletion of Dab1 phosphorylation sites. This result suggests that Dab1 phosphorylation is not related to the interaction

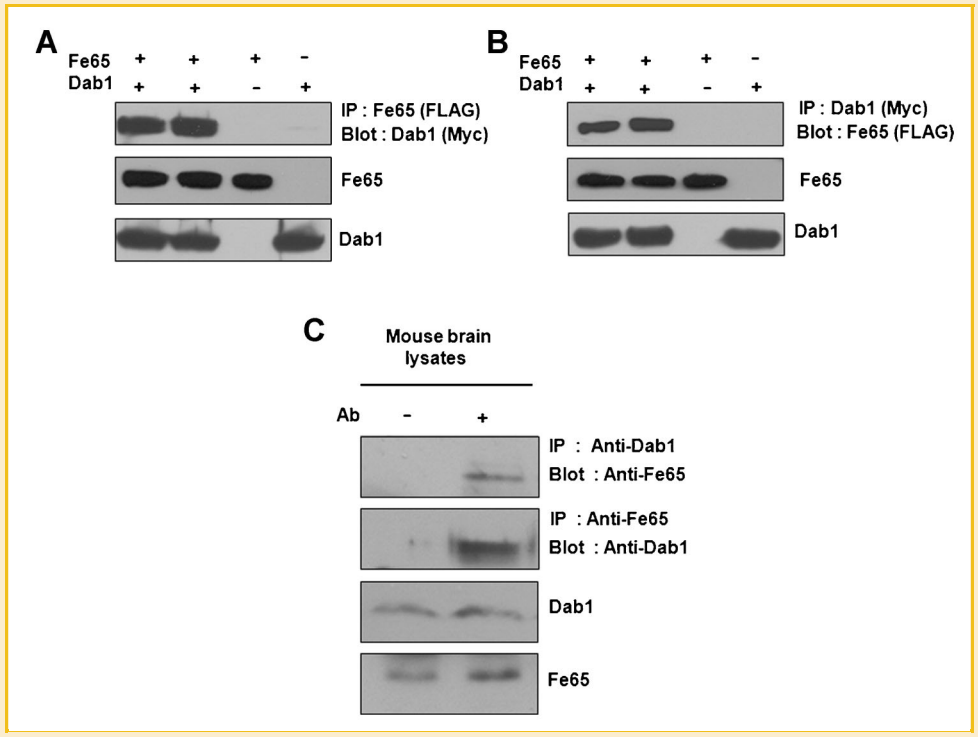

Fig. 3. Fe65 interacts with Dab1. A: HEK293 cells were co-transfected with Fe65 and Dab1 or each construct alone. Cell lysates were immunoprecipitated with anti-FLAG antibody, and the precipitate was probed with anti-Myc antibody. Dab1 was co-precipitated with Fe65 in HEK293 cells (upper panel). Immunoblots of cell lysates showed similar levels of Fe65 and Dab1 (middle and lower panels). B: The reverse experiment to (A) was performed. C: Mouse brain lysates were immunoprecipitated with anti-Dab1 antibody and probed with anti-Fe65 antibody (first panel). The reverse experiment was performed (second panel). (−) and (+) refer to the absence or presence of antibody in the immunoprecipitations. Immunoblots of brain lysates showed similar levels of Fe65 and Dab1 (lower panels).

with the Fe65, which may imply a different function from one in the Reelin pathway.

INTERACTIONS WITH Dab1 BINDERS DO NOT AFFECT THE Dab1 PHOSPHORYLATION

Tyrosine phosphorylation of Dab1 is important for its signal-transducing effects in development [Howell et al., 1999b]. In neuronal migration during development, the Dab1 protein functions downstream of the extracellular protein Reelin, binding to the receptors apoEr2 and very low-density lipoprotein (VLDL) receptor [Howell et al., 1999a]. The Reelin-receptor interaction activates the Src family kinases Src, Fyn, and Yes and stimulates Dab1 tyrosine phosphorylation through a Reelin-induced multimerization of the receptors. Reelin induced tyrosine phosphorylation of Dab1 relays Reelin cues inside migrating neurons by initiating a cascade of signaling events [Arnaud et al., 2003].

In order to examine whether the interaction of Dab1 with its binding partners affects the Dab1 phosphorylation, we co-transfected Dab1 with LRP, APP, and Fe65 in HEK293 cells with various combinations. Their lysates were immunoprecipitated with anti-Dab1 antibody, and the immunoprecipitants were then immunoblotted with anti-phosphotyrosine antibody. Dab1 bound all proteins but did not show anti-phosphotyrosine immunoreactivity on any condition (Fig. 5). This result shows that Dab1 binding LRP, APP, or Fe65 is not affecting to the phosphorylation of Dab1.

Dab1 DECREASES THE INTERACTION BETWEEN LRP AND APP, AFFECTING APP PROCESSING

The cytoplasmic adaptor protein Dab1 binds both LRP and APP intracellular domains, and potentially may affect the interaction of LRP with APP. To test whether Dab1 affects the interaction between LRP and APP, we determined the amount of APP co-precipitated with LRP in the absence or presence of Dab1. Dab1 significantly decreased co-precipitation of APP with LRP (Fig. 6A). The levels of LRP and APP expressions did not vary across the conditions. We next attempted to determine which part of Dab1 is leading to this effect. Because Dab1 interacts with LRP and APP through its PTB domain, we hypothesized that construct of Dab1 lacking the PTB domain would not affect the interaction between LRP and APP. As expected, Dab1-PTB significantly decreased co-precipitation of APP with LRP (Fig. 6B, lane 1). The deletion mutant of Dab1 without the PTB domain, Dab1-CTF did not affect the interaction between LRP and APP (Fig. 6B, lane 2). These results showed that Dab1 decreases the interaction between LRP and APP through its PTB domain.

The LRP-APP interaction plays a physiological role in APP processing [Pietrzik et al., 2004; Yoon et al., 2005]. LRP can promote Aβ production by altering the trafficking and processing of APP, possibly by APP/LRP interactions [Kounnas et al., 1995; Trommsdorff et al., 1998; Ulery et al., 2000; Pietrzik et al., 2002]. Absence of LRP or treatment of receptor-associated protein (RAP), an antagonist of all known LRP ligands, substantially reduced Aβ release [Ulery et al., 2000; Pietrzik et al., 2002]. Since our data showed that Dab1

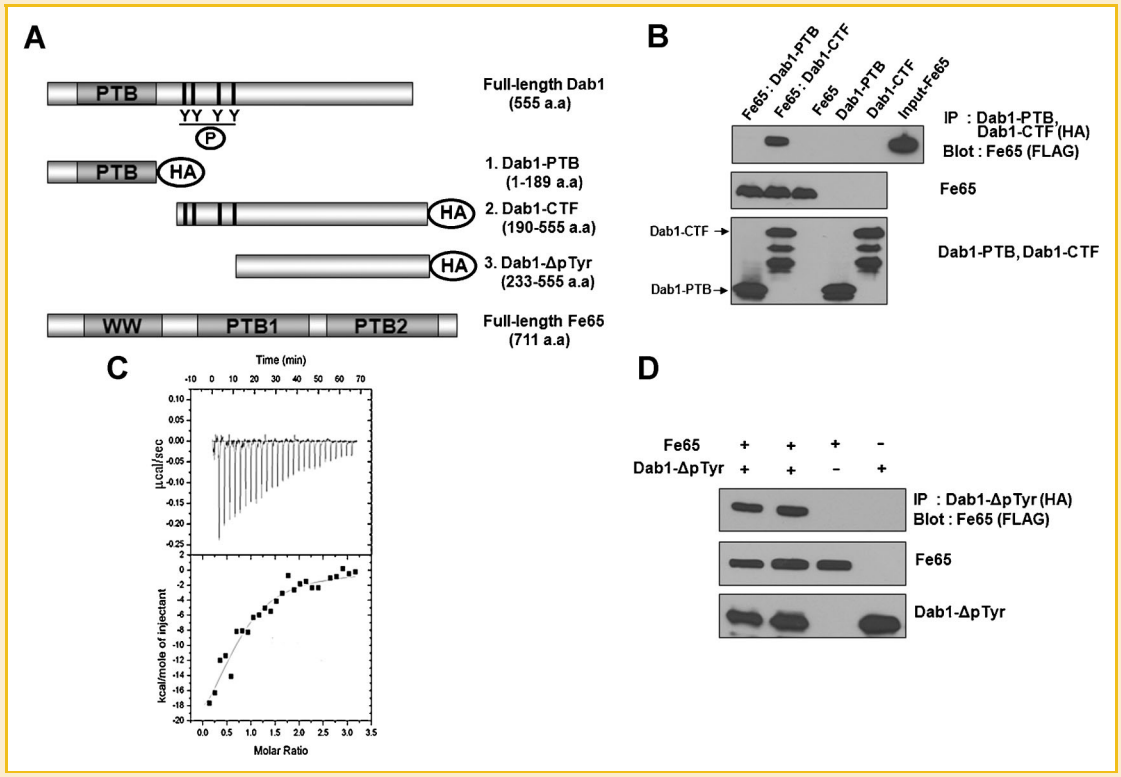

Fig. 4. The C-terminal region of Dab1 interacts with Fe65 and unphosphorylated Dab1 is capable of binding Fe65. A: Schematic representation of the PTB domain-containing adaptor proteins Dab1 and Fe65. WW, WW (tryptophan, tryptophan) protein interaction domain; PTB, phosphotyrosine-binding domain. The four tyrosine residues (198, 200, 220, and 232) in carboxyterminal of the Dab1 PTB domain are marked with a stretch of Y. Deletion mutants of C-terminal HA-tagged Dab1 were produced as follows: residues 1–189, PTB domain of Dab1 (Dab1-PTB); residues 190–555, PTB deletion construct of Dab1 (Dab1-CTF); residues 233–555, tyrosine phosphorylation sites deletion construct of Dab1 (Dab1-ΔpTyr). B: HEK293 cells were co-transfected with Fe65 and Dab1-PTB (lane 1), Fe65 and Dab1-CTF (lane 2), Fe65 (lane 3), Dab1-PTB (lane 4), Dab1-CTF (lane 5). Cell lysates were immunoprecipitated with anti-HA antibody, and the precipitate was probed with anti-FLAG antibody. Fe65 was co-precipitated with only Dab1-CTF (upper panel). Immunoblots of cell lysates showed similar levels of Fe65 and Dab1 deletion constructs (middle and lower panels). C: Isothermal titration calorimetry data for the in vitro interaction of Dab1-CTF and Fe65. A stock solution of the Dab1-CTF (150 μM) was added in 1.5 μl increments into a 10 μM solution of the Fe65. To calculate the dissociation constant, we fitted data to a one site binding model using the program Origin 7.0. D: HEK293 cells were co-transfected with Fe65 and Dab1-ΔpTyr or each construct alone. Cell lysates were immunoprecipitated with anti-HA antibody, and the precipitate was probed with anti-FLAG antibody. Fe65 was co-precipitated with Dab1-ΔpTyr (upper panel). Immunoblots of cell lysates showed similar levels of Fe65 and Dab1-ΔpTyr (middle and lower panels).

decreased the interaction between LRP and APP (Fig. 6A,B), we hypothesized that Dab1 might also affect processing of APP in the presence of LRP. To address this, the LRP was co-transfected into HEK293 cells with the APP and Dab1. Secreted APP was measured in conditioned media, and APP-CTF was measured in cell lysates. Compared with control medium, Dab1 overexpression decreased the levels of secreted APP and APP-CTF in LRP expressing cells, without affecting total levels of APP (Fig. 6C). This indicates that Dab1 decreases the levels of LRP–APP complex by interfering interaction, resulting in altered APP processing.

DISCUSSION

A number of studies have determined that small sequence motifs mediate protein–protein interactions and therefore are important for processing and function of proteins involved [Pawson and Scott, 1997]. One of the well-described interacting domain is the PTB domain [Parisiadou and Efthimiopoulos, 2007]. Adaptor proteins with PTB domains, such as X11, Fe65, JIP, and Dab, bind specifically to the C-terminal sequence YENPTY in the APP and affect trafficking and processing of APP [King and Scott Turner, 2004]. Because one motif of APP cytoplasmic domain is involved in the binding a couple of adaptor proteins, the competition of adaptor proteins is conceivable for binding to APP. Actually the competition between Fe65 and X11β or between Dab1 and X11α for binding to the APP has been reported [Lau et al., 2000; Parisiadou and Efthimiopoulos, 2007]. Dab1 affects the interaction of Fe65 with the cytoplasmic product of γ-secretase cleavage of APP-CTF, the APP intracellular domain (AICD) [Hoe et al., 2006b]. The effects of Dab1 on APP and apoEr2 could result from a competition between Dab1 and the other adaptor proteins binding to APP and apoEr2, preventing them from affecting trafficking and processing [Hoe et al., 2006b]. Therefore, it is very plausible that Fe65 and Dab1 compete for binding to APP in cells. APP did not tether Fe65 in cytoplasm when Dab1 and Fe65 were co-transfected with APP (Fig. 1C, a–d). In addition, the amount of Fe65 bound to APP was decreased in the presence of Dab1 (Fig. 2A). On the other hand, the amount of Dab1 bound to APP was

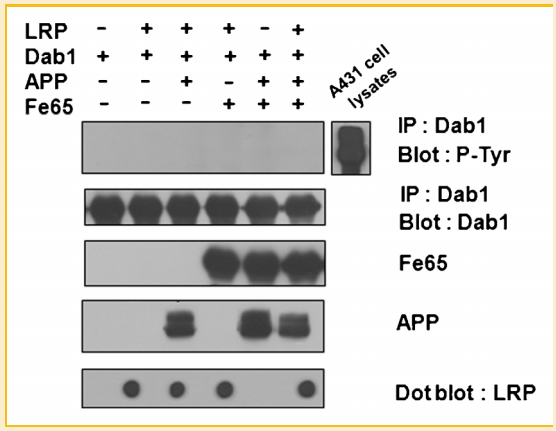

Fig. 5. The Dab1 binding proteins do not affect the phosphorylation of Dab1. HEK293 cells were co-transfected with Dab1 (lane 1), LRP and Dab1 (lane 2), LRP, Dab1 and APP (lane 3), LRP, Dab1 and Fe65 (lane 4), Dab1, APP and Fe65 (lane 5), LRP, Dab1, APP and Fe65 (lane 6). Cell lysates were immunoprecipitated with anti-Dab1 antibody, and the precipitate was probed with an anti-phosphotyrosine (P-Tyr) antibody or anti-Dab1 antibody. Dab1 did not show anti-phosphotyrosine immunoreactivity (top panel). Lysates from co-transfected cells were probed for APP, Fe65, or LRP to demonstrate expression levels (lower panels). EGF-stimulated A431 cell lysate is provided as a positive antigen control for Western blotting.

decreased in the presence of Fe65 (Fig. 2B). These results indicate that Dab1 and Fe65 compete for binding to APP.

Fe65 has been reported by many groups to form a transcriptionally active complex with APP/AICD in heterologous gene reporter systems [Cao and Sudhof, 2001, 2004; Kimberly et al., 2001]. It seems most likely that APP serves to tether Fe65 to cytoplasmic membranes [Minopoli et al., 2001]. After γ-secretase cleavage, an AICD/Fe65 complex is released allowing AICD and Fe65 to translocate to the nucleus and to participate in gene transcription events either together or separately [McLoughlin and Miller, 2008]. The precise mechanism regulating these events is not yet clear. Our results may imply a way to modulate the translocation of Fe65 to the nucleus. The interaction between Fe65 and APP was reduced by competing for binding with Dab1 when they exist together. APP could not tether Fe65 in the cytoplasm by the interaction between Dab1 and APP. Thus, Fe65 can be released from the cytoplasm without cleavage by γ-secretase activity, and translocated to the nucleus to be involved in gene transcription. How the translocation of Fe65 affects to the next steps of this regulation needs further investigations.

Several studies have shown that interactions between adaptor proteins and APP lead to altered processing of APP [Hoe et al., 2006a]. X11α/Mint-1 delays maturation of APP, increases its half-life, and reduces the production of Aβ [Borg et al., 1996; Miller et al., 2006]. SNX17 is an early endosomal protein that facilitates APP recycling to the cell surface, as reduction of SNX17 decreased APP half-life and increased Aβ production [Lee et al., 2008]. The c-*jun* N-terminal kinase (JNK) interacting proteins (JIPs) interaction with APP stabilizes immature APP and inhibits APPs, Aβ production [Taru et al., 2002]. We have investigated the effect of Fe65 and Dab1 co-expression on the APP processing. Interestingly, we observed that Fe65 and Dab1 exert opposing effects on the secretion of APP and the levels of APP-CTF (Fig. 2C). When Fe65 and Dab1 were co-expressed, we did not detect an increase in the secreted APP but partly restored levels of secreted APP compared with the cells expressing Fe65. It has been reported that Fe65 stabilizes immature APP and inhibits APPs formation and Aβ secretion [Ando et al., 2001]. Recent studies showed that Dab1 interaction with APP and apoEr2 increases levels of their secreted extracellular domains and cytoplasmic C-terminal fragments [Hoe et al., 2006b]. It is possible that modulation of APP metabolism and subsequent Aβ production by these proteins depends on their competition for binding to APP, at least partially. This should be carefully studied more, since the binding to APP of Fe65 or Dab1 is reduced to about a half by co-expression, but co-expression results in different degrees of effect on APP secretion by Fe65 and Dab1 (Fig. 2). Also, the co-expression affects to the translocation of Fe65 that could cause the change in gene transcription.

Binding partners for the Fe65 proteins have been reported, which are proving informative about their functions [McLoughlin and Miller, 2008]. Co-expression of Fe65 with Dab1 did not affect nuclear translocation of Fe65 (Fig. 1A, k–m and B). However, we surprisingly found the interaction between Fe65 and Dab1 (Fig. 3). Co-immunoprecipitation with various deletion mutants of Dab1 demonstrated that Fe65 interact with Dab1 in cells (Fig. 4). This interaction occurs via C-terminal region of Dab1 but not PTB domain of Dab1. This seems reasonable since the PTB domain may be involved in the regulation of binding partners, so the rest can work with other adaptor proteins for the additional regulation or the other functions. The role of tyrosine phosphorylation sites in the C-terminal region of Dab1 on the interaction with Fe65 was examined. The CrkII–Dab1 interaction requires tyrosine phosphorylation of Dab1 at residues 220 or 232 and is promoted by Reelin treatment [Chen et al., 2004]. The SH2 domain of Nckβ but not Nckα binds Dab1 phosphorylated on Y220 or Y232 [Pramatarova et al., 2003]. In addition, Dab1 interacts with Lis1, a protein with no SH2 domain, in manner that depends on Dab1 phosphorylation at Y198 or Y220 [Assadi et al., 2003]. Dab1 phosphorylation was not required for the interaction with the Fe65 (Fig. 4D). This may imply that the binding to Fe65 is related to a different function of Dab1 rather than phosphorylation-dependent signal transduction.

After examining which domain of Dab1 interacted with Fe65, we examined which domain of Fe65 interacted with Dab1. In addition to full-length Fe65, we checked deletion mutants of the WW and PTB1 domains, only the PTB1 domain, and the PTB1 and PTB2 domains. We found that all three constructs could not interact with Dab1 (data not shown). These results may hint that only full-length Fe65 can interact with Dab1 and all three domains of Fe65 are involved in the binding to Dab1. The interaction of Fe65 with Dab1 may induce the conformational change or modification of Fe65 molecule. The conformational change of Fe65 was proposed in a previous report that Fe65 is liberated from membrane by γ-cleavage of APP as a complex including AICD [Cao and Sudhof, 2004]. Considering our data, the binding of Dab1 might induce a kind of closed conformation of WW and the PTB domains in Fe65. The closed conformation of Fe65 may affect to the interaction with APP, and to Fe65 translocation into nucleus for gene transactivation. This

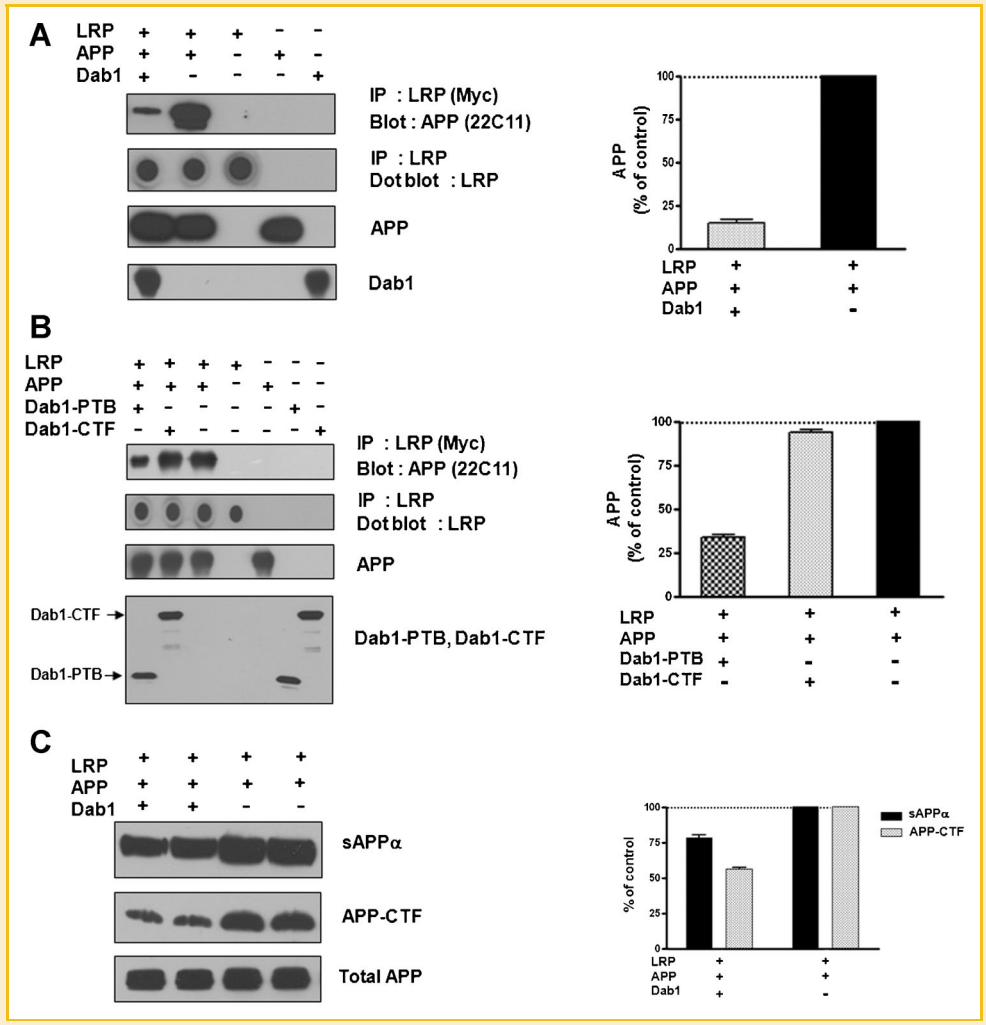

Fig. 6. Dab1 decreased the binding of APP and LRP. A: HEK293 cells were co-transfected with LRP, APP and Dab1 (lane 1), LRP and APP (lane 2), LRP (lane 3), APP (lane 4), Dab1 (lane 5). Cell lysates were immunoprecipitated with anti-Myc antibody, and the precipitate was probed with 22C11 antibody. Dab1 decreased co-precipitation of APP and LRP (top panel). Immunoblots of cell lysates showed similar levels of total APP and LRP (lower panels). Three independent experiments were performed and the standard deviations were calculated for the quantification graph of the blot. B: HEK293 cells were co-transfected with LRP, APP and Dab1-PTB (lane 1), LRP, APP and Dab1-CTF (lane 2), LRP and APP (lane 3), LRP (lane 4), APP (lane 5), Dab1-PTB (lane 6), Dab1-CTF (lane 7). Cell lysates were immunoprecipitated with anti-Myc antibody, and the precipitate was probed with 22C11 antibody. Dab1-PTB decreased co-precipitation of APP and LRP (top panel). Immunoblots of cell lysates showed similar levels of total APP and LRP (lower panels). Three independent experiments were performed and the standard deviations were calculated for the quantification graph of the blot. C: Dab1 alters APP processing in the presence of LRP. HEK293 cells were co-transfected with LRP and APP without or with Dab1. Secreted APPα was measured in conditioned medium with 6E10 antibody (upper panel), and APP-CTF was measured in cell lysates with 8717 antibody (middle panel). Immunoblot of cell lysates showed similar levels of total APP (lower panel). Three independent experiments were performed and the standard deviations were calculated for the quantification graph of the blot.

newly found interaction among adaptor proteins should be investigated further for the detailed mechanism affecting APP trafficking and processing.

LRP and APP are linked by two PTB domains of Fe65; the presence of Fe65 increases the interaction between LRP and APP [Pietrzik et al., 2004]. Previous studies reported that in LRP expressing cells, Fe65 overexpression resulted in an approximate two- to threefold increase in APPs secretion compared to mock transfected cells. Overexpression of Fe65 should influence APP processing by altering the levels of APP–LRP complex [Pietrzik et al., 2004]. Dab1 interacts with both LRP and APP through its PTB domain [Hoe et al., 2006b]. Our data show that Dab1 significantly decreased the amount of APP bound to LRP (Fig. 6A,B). Overexpression of Dab1 in LRP expressing cells also decreased the level of secreted APP and APP-CTF compared to untransfected control cells (Fig. 6C). These results suggested that overexpression of Dab1 acted in a negative manner, possibly by reducing the amount of LRP complexed to APP. In view of previous results demonstrating that the distal NPXY motif of LRP appeared to be critical for APP processing, it may be that the interaction with second NPXY motif between Fe65 and LRP is physiologically more important [Pietrzik et al., 2002, 2004]. It is also known that Dab1 binds to the second NPXY motif of LRP [Trommsdorff et al., 1998]. Dab1 and Fe65 exert opposing effects on the interaction between LRP and APP, and APP

processing. Dab1 could prevent the Fe65 intracellular link between LRP and APP, probably by competing for binding to the NPXY motifs of LRP and APP or binding to Fe65 itself. Dab1 binds to the 14-mer ApoEr2 NPXY peptide that has a very similar sequence to the LRP motif with 1–2 μM of Kd [Stolt et al., 2003]. Dab1 PTB domain also has a similar affinity toward 17-mer APP peptide [Howell et al., 1999b]. Interestingly, PTB2 domain of Fe65 showed much weaker affinity of ~100 μM (Kd) when the shorter 11-mer APP peptide bound to it, but ~0.2 μM with the longer 32–50-mer peptides [Radzimanowski et al., 2008]. The Kd between Dab1-CTF and Fe65 was ~5.8 μM. These biochemical data suggest sets of experiments with full-length proteins in vivo, preferably in a natural system containing all players of this regulation mechanism in order to know the exact effects of each protein. Understanding the competitive mechanisms of intracellular adaptor proteins which might be working by subtle changes will be vital in describing the regulation of interacting proteins like LRP and APP.

ACKNOWLEDGMENTS

We thank Dr. J. Herz (UT Southwestern, USA), Dr. P. Stolt-Bergner (Research Institute of Molecular Pathology, Austria), Dr. K. Min (LGLS Co., Korea) for kindly giving plasmids of LRP, Dab1, and APP. This work was supported by a KIST Institutional Grant, and by Molecular Imaging and GRL "Theragnosis" grants from the Korean Government (MEST).

REFERENCES

Ando K, Iijima KI, Elliott JI, Kirino Y, Suzuki T. 2001. Phosphorylation-dependent regulation of the interaction of amyloid precursor protein with Fe65 affects the production of beta-amyloid. J Biol Chem 276:40353–40361.

Arnaud L, Ballif BA, Cooper JA. 2003. Regulation of protein tyrosine kinase signaling by substrate degradation during brain development. Mol Cell Biol 23:9293–9302.

Assadi AH, Zhang G, Beffert U, McNeil RS, Renfro AL, Niu S, Quattrocchi CC, Antalffy BA, Sheldon M, Armstrong DD, Wynshaw-Boris A, Herz J, D'Arcangelo G, Clark GD. 2003. Interaction of reelin signaling and Lis1 in brain development. Nat Genet 35:270–276.

Bar I, Lambert de Rouvroit C, Goffinet AM. 2000. The Reelin signaling pathway in mouse cortical development. Eur J Morphol 38:321–325.

Borg JP, Ooi J, Levy E, Margolis B. 1996. The phosphotyrosine interaction domains of X11 and FE65 bind to distinct sites on the YENPTY motif of amyloid precursor protein. Mol Cell Biol 16:6229–6241.

Cao X, Sudhof TC. 2001. A transcriptionally [correction of transcriptively] active complex of APP with Fe65 and histone acetyltransferase Tip60. Science 293:115–120.

Cao X, Sudhof TC. 2004. Dissection of amyloid-beta precursor protein-dependent transcriptional transactivation. J Biol Chem 279:24601–24611.

Chang Y, Tesco G, Jeong WJ, Lindsley L, Eckman EA, Eckman CB, Tanzi RE, Guenette SY. 2003. Generation of the beta-amyloid peptide and the amyloid precursor protein C-terminal fragment gamma are potentiated by FE65L1. J Biol Chem 278:51100–51107.

Chen K, Ochalski PG, Tran TS, Sahir N, Schubert M, Pramatarova A, Howell BW. 2004. Interaction between Dab1 and CrkII is promoted by Reelin signaling. J Cell Sci 117:4527–4536.

Ermekova KS, Zambrano N, Linn H, Minopoli G, Gertler F, Russo T, Sudol M. 1997. The WW domain of neural protein FE65 interacts with proline-rich motifs in Mena, the mammalian homolog of Drosophila enabled. J Biol Chem 272:32869–32877.

Gandy S. 2005. The role of cerebral amyloid beta accumulation in common forms of Alzheimer disease. J Clin Invest 115:1121–1129.

Gotthardt M, Trommsdorff M, Nevitt MF, Shelton J, Richardson JA, Stockinger W, Nimpf J, Herz J. 2000. Interactions of the low density lipoprotein receptor gene family with cytosolic adaptor and scaffold proteins suggest diverse biological functions in cellular communication and signal transduction. J Biol Chem 275:25616–25624.

Guenette SY, Chen J, Ferland A, Haass C, Capell A, Tanzi RE. 1999. hFE65L influences amyloid precursor protein maturation and secretion. J Neurochem 73:985–993.

Guenette SY, Chang Y, Hyman BT, Tanzi RE, Rebeck GW. 2002. Low-density lipoprotein receptor-related protein levels and endocytic function are reduced by overexpression of the FE65 adaptor protein, FE65L1. J Neurochem 82:755–762.

Herz J, Strickland DK. 2001. LRP: A multifunctional scavenger and signaling receptor. J Clin Invest 108:779–784.

Hoe HS, Rebeck GW. 2008. Functional interactions of APP with the apoE receptor family. J Neurochem 106:2263–2271.

Hoe HS, Wessner D, Beffert U, Becker AG, Matsuoka Y, Rebeck GW. 2005. F-spondin interaction with the apolipoprotein E receptor ApoEr2 affects processing of amyloid precursor protein. Mol Cell Biol 25:9259–9268.

Hoe HS, Magill LA, Guenette S, Fu Z, Vicini S, Rebeck GW. 2006a. FE65 interaction with the ApoE receptor ApoEr2. J Biol Chem 281:24521–24530.

Hoe HS, Tran TS, Matsuoka Y, Howell BW, Rebeck GW. 2006b. DAB1 and Reelin effects on amyloid precursor protein and ApoE receptor 2 trafficking and processing. J Biol Chem 281:35176–35185.

Honda T, Nakajima K. 2006. Mouse Disabled1 (DAB1) is a nucleocytoplasmic shuttling protein. J Biol Chem 281:38951–38965.

Howell BW, Gertler FB, Cooper JA. 1997a. Mouse disabled (mDab1): A Src binding protein implicated in neuronal development. EMBO J 16:121–132.

Howell BW, Hawkes R, Soriano P, Cooper JA. 1997b. Neuronal position in the developing brain is regulated by mouse disabled-1. Nature 389:733–737.

Howell BW, Herrick TM, Cooper JA. 1999a. Reelin-induced tyrosine [corrected] phosphorylation of disabled 1 during neuronal positioning. Genes Dev 13:643–648.

Howell BW, Lanier LM, Frank R, Gertler FB, Cooper JA. 1999b. The disabled 1 phosphotyrosine-binding domain binds to the internalization signals of transmembrane glycoproteins and to phospholipids. Mol Cell Biol 19:5179–5188.

Howell BW, Herrick TM, Hildebrand JD, Zhang Y, Cooper JA. 2000. Dab1 tyrosine phosphorylation sites relay positional signals during mouse brain development. Curr Biol 10:877–885.

Kimberly WT, Zheng JB, Guenette SY, Selkoe DJ. 2001. The intracellular domain of the beta-amyloid precursor protein is stabilized by Fe65 and translocates to the nucleus in a notch-like manner. J Biol Chem 276:40288–40292.

King GD, Scott Turner R. 2004. Adaptor protein interactions: Modulators of amyloid precursor protein metabolism and Alzheimer's disease risk? Exp Neurol 185:208–219.

Kinoshita A, Whelan CM, Smith CJ, Mikhailenko I, Rebeck GW, Strickland DK, Hyman BT. 2001. Demonstration by fluorescence resonance energy transfer of two sites of interaction between the low-density lipoprotein receptor-related protein and the amyloid precursor protein: Role of the intracellular adapter protein Fe65. J Neurosci 21:8354–8361.

Kinoshita A, Whelan CM, Smith CJ, Berezovska O, Hyman BT. 2002. Direct visualization of the gamma secretase-generated carboxyl-terminal domain of the amyloid precursor protein: Association with Fe65 and translocation to the nucleus. J Neurochem 82:839–847.

Kounnas MZ, Moir RD, Rebeck GW, Bush AI, Argraves WS, Tanzi RE, Hyman BT, Strickland DK. 1995. LDL receptor-related protein, a multifunctional

ApoE receptor, binds secreted beta-amyloid precursor protein and mediates its degradation. Cell 82:331–340.

Lau KF, McLoughlin DM, Standen CL, Irving NG, Miller CC. 2000. Fe65 and X11beta co-localize with and compete for binding to the amyloid precursor protein. Neuroreport 11:3607–3610.

Lee J, Retamal C, Cuitino L, Caruano-Yzermans A, Shin JE, van Kerkhof P, Marzolo MP, Bu G. 2008. Adaptor protein sorting nexin 17 regulates amyloid precursor protein trafficking and processing in the early endosomes. J Biol Chem 283:11501–11508.

Li H, Koshiba S, Hayashi F, Tochio N, Tomizawa T, Kasai T, Yabuki T, Motoda Y, Harada T, Watanabe S, Inoue M, Hayashizaki Y, Tanaka A, Kigawa T, Yokoyama S. 2008. Structure of the C-terminal phosphotyrosine interaction domain of Fe65L1 complexed with the cytoplasmic tail of amyloid precursor protein reveals a novel peptide binding mode. J Biol Chem 283:27165–27178.

McLoughlin DM, Miller CC. 2008. The FE65 proteins and Alzheimer's disease. J Neurosci Res 86:744–754.

Miller CC, McLoughlin DM, Lau KF, Tennant ME, Rogelj B. 2006. The X11 proteins, Abeta production and Alzheimer's disease. Trends Neurosci 29: 280–285.

Minopoli G, de Candia P, Bonetti A, Faraonio R, Zambrano N, Russo T. 2001. The beta-amyloid precursor protein functions as a cytosolic anchoring site that prevents Fe65 nuclear translocation. J Biol Chem 276:6545–6550.

Parisiadou L, Efthimiopoulos S. 2007. Expression of mDab1 promotes the stability and processing of amyloid precursor protein and this effect is counteracted by X11alpha. Neurobiol Aging 28:377–388.

Pawson T, Scott JD. 1997. Signaling through scaffold, anchoring, and adaptor proteins. Science 278:2075–2080.

Pietrzik CU, Busse T, Merriam DE, Weggen S, Koo EH. 2002. The cytoplasmic domain of the LDL receptor-related protein regulates multiple steps in APP processing. EMBO J 21:5691–5700.

Pietrzik CU, Yoon IS, Jaeger S, Busse T, Weggen S, Koo EH. 2004. FE65 constitutes the functional link between the low-density lipoprotein receptor-related protein and the amyloid precursor protein. J Neurosci 24:4259–4265.

Pramatarova A, Ochalski PG, Chen K, Gropman A, Myers S, Min KT, Howell BW. 2003. Nck beta interacts with tyrosine-phosphorylated disabled 1 and redistributes in Reelin-stimulated neurons. Mol Cell Biol 23:7210–7221.

Radzimanowski J, Simon B, Sattler M, Beyreuther K, Sinning I, Wild K. 2008. Structure of the intracellular domain of the amyloid precursor protein in complex with Fe65-PTB2. EMBO Rep 9:1134–1140.

Sabo SL, Ikin AF, Buxbaum JD, Greengard P. 2001. The Alzheimer amyloid precursor protein (APP) and FE65, an APP-binding protein, regulate cell movement. J Cell Biol 153:1403–1414.

Santiard-Baron D, Langui D, Delehedde M, Delatour B, Schombert B, Touchet N, Tremp G, Paul MF, Blanchard V, Sergeant N, Delacourte A, Duyckaerts C, Pradier L, Mercken L. 2005. Expression of human FE65 in amyloid precursor protein transgenic mice is associated with a reduction in beta-amyloid load. J Neurochem 93:330–338.

Stolt PC, Bock HH. 2006. Modulation of lipoprotein receptor functions by intracellular adaptor proteins. Cell Signal 18:1560–1571.

Stolt PC, Jeon H, Song HK, Herz J, Eck MJ, Blacklow SC. 2003. Origins of peptide selectivity and phosphoinositide binding revealed by structures of disabled-1 PTB domain complexes. Structure 11:569–579.

Taru H, Kirino Y, Suzuki T. 2002. Differential roles of JIP scaffold proteins in the modulation of amyloid precursor protein metabolism. J Biol Chem 277: 27567–27574.

Trommsdorff M, Borg JP, Margolis B, Herz J. 1998. Interaction of cytosolic adaptor proteins with neuronal apolipoprotein E receptors and the amyloid precursor protein. J Biol Chem 273:33556–33560.

Ulery PG, Beers J, Mikhailenko I, Tanzi RE, Rebeck GW, Hyman BT, Strickland DK. 2000. Modulation of beta-amyloid precursor protein processing by the low density lipoprotein receptor-related protein (LRP). Evidence that LRP contributes to the pathogenesis of Alzheimer's disease. J Biol Chem 275: 7410–7415.

Yoon IS, Pietrzik CU, Kang DE, Koo EH. 2005. Sequences from the low density lipoprotein receptor-related protein (LRP) cytoplasmic domain enhance amyloid beta protein production via the beta-secretase pathway without altering amyloid precursor protein/LRP nuclear signaling. J Biol Chem 280:20140–20147.